Volume 1 | Number 1 | Jan 2013 | Pages 1–100

## Soft Matter

www.rsc.org/softmatter

ROYAL SOCIETY
OF CHEMISTRY

ROYAL SOCIETY
OF CHEMISTRY

www.rsc.org/softmatter

# Journal Name

## ARTICLE

## Celebrating *Soft Matter's* 10th Anniversary: Screening calcium-induced spontaneous curvature of lipid membranes

Mijo Simunovic,[a,b] Ka Yee C. Lee[b] and Patricia Bassereau[a]

Lipid membranes are key regulators of cellular function. An important step in membrane-related phenomena is the reshaping of the lipid bilayer, often induced by binding of macromolecules. Numerous experimental and simulation efforts have revealed that calcium, a ubiquitous cellular messenger, has a strong impact on the phase behavior, structural properties, and the stability of membranes. Yet, it is still unknown the way interactions of calcium with lipids affect their macroscopic mechanical properties. In this work, we studied the interaction of calcium ions with membrane tethers pulled from giant unilamellar vesicles, to quantify the mechanical effect on the membrane. We found that calcium imposes a positive spontaneous curvature in negatively charged membranes, contrary to predictions we made based on the proposed atomic structure. Surprisingly, this effect vanishes in the presence of physiologically relevant concentrations of sodium chloride. Our work implies that calcium may be a trigger of membrane reshaping only at high concentrations, in a process that is robustly screened by sodium ions.

## Notes and references

*a* Institut Curie, Centre National de la Recherche Scientifique, Unité Mixte de Recherche 168, Université Pierre et Marie Curie, F-75248 Paris, France.
*b* Department of Chemistry, Institute for Biophysical Dynamics, and James Franck Institute, The University of Chicago, 60637 Illinois, USA.
Correspondence: patricia.bassereau@curie.fr

## Introduction

Calcium ion is a major signaling species that takes part in numerous cellular processes[1]. It significantly alters the local electrostatics of macromolecules and, by doing so, it can trigger a conformational change in some proteins[2, 3]. Being a powerful cellular messenger, its equilibrium cytosolic concentration is kept four orders of magnitude lower than outside the cell, at $\sim$ 100 nM[1]. Calcium also interacts with lipid membranes, which may drive large-scale morphological transformations, such as membrane fusion[4].

The effect of calcium on lipid membranes has been studied for decades. Early on, it was shown that calcium couples with the phase behavior, structural properties, and the stability of bilayers[5-7]. More lately, tremendous experimental and simulation efforts have been taken to elucidate the interactions of calcium with lipid bilayers, in light of significantly varying views on the precise atomic aspects of this phenomenon[8, 9]. This variation is often attributed to the measuring methodology or experimental conditions, such as the concentration of calcium or other ions[8].

Studies on monolayers composed of phosphatidylinositol 4,5-bisphosphate ($PIP_2$) revealed that ions have a marked effect on the organization of lipids. Specifically, monovalent cations induce the expansion of $PIP_2$ monolayers, while divalent cations compress them[10]. The same authors did not observe an appreciable effect of $Na^+$ on phosphatidylserine (PS) monolayers, although others have reported a reduction of lipid area upon $Ca^{2+}$ binding to PS-containing bilayers[9, 11]. Simulations have shown that $Na^+$ penetrates deep into the bilayer[12-14]. Calcium ions, on the other hand, seem to be coordinated at the level of the phosphate group in both PS and $PIP_2$ membranes[15, 16]. This structural arrangement and the reported dehydration of the bilayer upon calcium binding[8, 17] most likely results in the tighter packing of lipids leading to a reduction in the lipid area.

Binding of calcium may even drive the formation of heterogeneities in the lateral composition of the membrane. In particular, studies have shown calcium-induced clustering of $PIP_2$ in monolayers and bilayers composed of phosphatidylcholine (PC) and $PIP_2$[10, 16]. Moreover, calcium causes demixing of PS-containing monolayers at lower lateral pressure[11].

In light of the numerous effects calcium can impart on the membrane, it is expected that its binding leads to macroscopic changes in the structure of the bilayer. However, it is still unclear whether $Ca^{2+}$ affects the mechanical and morphological

properties of the membrane, such as bending rigidity or the spontaneous curvature. Cell membranes in great part comprise PC and PS lipids, especially in the cytosolic leaflet[18], therefore it is of key importance to understand all aspects of how this ubiquitous signaling ion interacts with PS-containing membranes. Our aim in this work is to investigate and quantify the mechanical effect of $Ca^{2+}$ ions on mixed PC/PS model membranes.

## Results and Discussion

A membrane at equilibrium will take a shape that corresponds to its spontaneous curvature. If a bilayer has homogeneously distributed lipids and equal composition in both layers, its spontaneous curvature is zero. Binding of particles may impose an asymmetry in the bilayer that leads to a nonzero spontaneous curvature[19]. We define positive curvature when the membrane curves toward the binding leaflet and negative otherwise (Fig. 1A).
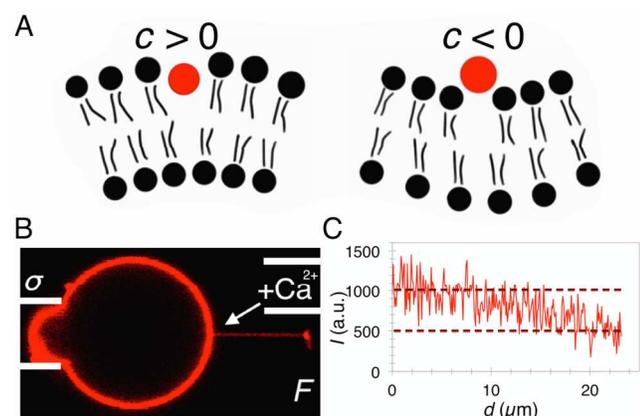


**Fig 1 (A)** A scheme of a lipid bilayer with positive (left) and negative (right) spontaneous curvature (*c*). $Na^+$ dilates the lipid leaflet and is expected to induce positive curvature, while $Ca^{2+}$ compresses lipids and so it should induce negative curvature. **(B)** A scheme of a tether-pulling experiment. Aspiration pipette controls membrane tension ($\sigma$), while the remodeling force ($F$) is measured from the displacement of the bead in the optical trap. We use another pipette to inject $Ca^{2+}$. **(C)** Dilution of the injected solution from the injection pipette exit to the base of the membrane tether, measured from fluorescence intensity of a labeled molecule. The plot shows one out of three measurements.

Based on experimental and simulation evidence, monovalent cations insert between the lipids and dilate the membrane. Considering that, this way, lipids prefer to be further apart from one another, we expect this process to induce a positive spontaneous curvature (Fig. 1A, left). Conversely, as calcium contracts the lipid bilayer, it could lead to negative spontaneous curvature where lipids in the calcium-binding leaflet are closer to one another (Fig. 1A, right).

To study this effect, we used a giant unilamellar vesicle (GUV) as a model membrane. By changing the pressure in the aspiration micropipette holding the GUV, we control its surface tension. We used a micron-sized bead, trapped with optical

tweezers, to pull a tether from the GUV. Based on the movement of the bead, we track, in time, the retraction force of the tether. This force effectively represents the remodeling force of the membrane. Finally, with another pipette, we inject a $Ca^{2+}$ solution in the vicinity of the system (Fig. 1B). We refer the reader to our previous work where we have shown that this method is very sensitive to detecting spontaneous curvature, evidenced by a sudden change in the tether-retraction force upon the injection of curvature-inducing molecules[20, 21].

An important advantage of injecting calcium solution directly onto the GUV and not pre-incubating the GUV is that we can compare the behavior in the absence and the presence of the ion on the same vesicle. Additionally, high bulk $Ca^{2+}$ concentrations would induce undesirable fusion between vesicles. However, the concentration inside the pipette is not the same as the concentration in the vicinity of the membrane tether due to dilution. Therefore, we first determined how much of the injected solution is diluted. We injected a fluorescent marker linked to a membrane-binding protein and measured the fluorescence intensity from the exit of the injection pipette to the GUV (see Materials and Methods). We found that the concentration of the injected solution is on average halved at the tether-GUV interface (Fig. 1C) and so, in the following calculations, we corrected the bulk calcium concentrations accordingly.

We carried out experiments on three different lipid compositions: 1) DOPC; 2) DOPC:DOPS (9:1); and 3) DOPC:DOPS (8:2). We did not test membranes with higher net charge, as physiologically relevant concentration of PS lipids is in the 10–20% range[22]. Unexpectedly, the tether retraction force did not deviate when injecting 10 mM $Ca^{2+}$ on a 20% DOPS GUV (Fig. 2A). In addition, we could not observe a difference in the retraction force compared to a bare membrane at a wide range of surface tensions, up to 0.2 mN/m (Fig. 2B). To ensure that $Ca^{2+}$ binding is not dependent on the direction of change of membrane tension, we confirmed that the forces superimpose whether stepwise increasing or decreasing tension (Fig. 2B, red and maroon dots). If binding of $Ca^{2+}$ would induce negative curvature, the bilayer would tend to curve away from the binding leaflet and thus oppose the positive curvature of the membrane tether. Hence, we would expect an increase in the tether retraction force.

Moreover, nonzero spontaneous curvature would affect the equilibrium radius of the pulled tether, compared to a reference membrane at the same membrane tension. We computed the radius of the tether from the measured lipid fluorescence intensity (see Materials and Methods) and found no difference in the presence or absence of $Ca^{2+}$ on 20% PS membranes (Fig. 2B).

Before discussing the implications of these results, we quantify the mechanical properties of the membrane. First, we derive the relationship between force, radius, and tension from the Helfrich Hamiltonian[19]:

$$H_t = \frac{\kappa}{2}\left(\frac{1}{r} - \frac{1}{R_0}\right)^2 A + \sigma A - fL \tag{1}$$

$H_t$ is the total free energy of the tether, $\kappa$ is the membrane bending rigidity, $r$ and $R_0$ are respectively the mean and the spontaneous radii of curvature, $A$ and $L$ are respectively the area and the length of the tether, and $f$ is the pulling force on the membrane. At equilibrium, $r$ becomes the tether radius ($R$) and the force becomes the aforementioned tether retraction force ($F$). To compute $R$ and $F$, we minimize $H_t$ with respect to $L$ and $R^{(23)}$, i.e. $\partial H_t / \partial R = 0$ and $\partial H_t / \partial L = 0$, yielding,

$$F \approx 2\pi\sqrt{2\kappa\sigma} - 2\pi\kappa\frac{1}{R_0} \tag{2}$$

$$\frac{1}{R^2} = \frac{2\sigma}{\kappa} + \frac{1}{R_0^2} \tag{3}$$

The equations reveal that the tether curvature and the tether-retraction force scale as square root of membrane tension. Fitting the model to our data gives $\kappa$ and $R_0$. Considering that we measured the radius from the fluorescence intensity, we have two independent measurements of $\kappa$ and $R_0$. We note that we cannot predict the direction of curvature from Eq. 3 since $R_0$ appears as a square.

Just like in the two GUVs presented in Figure 2 (A and B), we did not detect an appreciable difference in the radius or the force in the presence of up to 50 mM $Ca^{2+}$ for any of the three membrane compositions, at a relatively wide range of membrane tensions, up to ~0.3 mN/m (Fig. 2C).
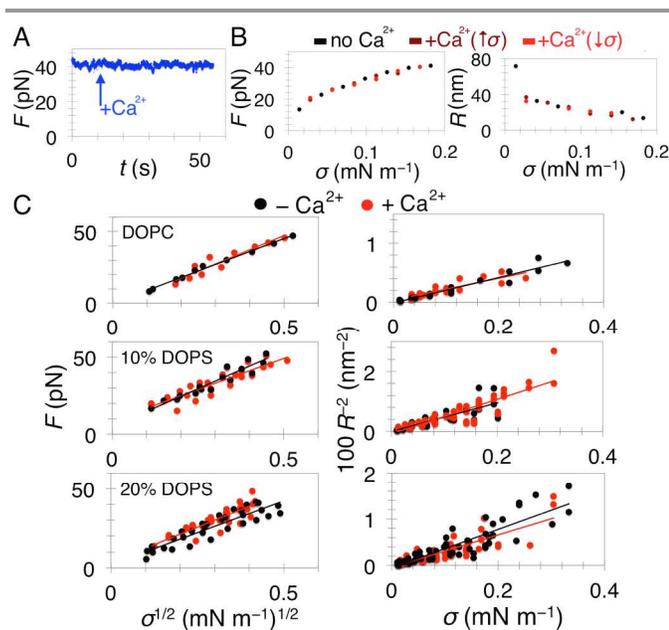


**Fig 2** The mechanics of DOPC and DOPC/DOPS membranes in the presence of NaCl and $Ca^{2+}$. (**A**) $F$ as a function of time ($t$) during injection of 10 mM $Ca^{2+}$ to a DOPC:DOPS = 8:2 GUV in 100 mM NaCl buffer. (**B**) $F$ and $R$ as a function of $\sigma$ for a DOPC:DOPS = 8:2 GUV in 100 mM NaCl buffer (different example from $A$). First, the measurement was done in the absence of $Ca^{2+}$ (black dots) by step-wise increasing $\sigma$. Then, $\sigma$ was reduced to a minimum and the measurement was repeated with 10 mM $Ca^{2+}$ (maroon dots). Finally, continuing to inject, the measurement was repeated, but the tension was stepwise reduced (red dots). (**C**) Uncharged membrane displays no spontaneous curvature (top), while charged membranes show weak negative spontaneous curvature (centre and bottom). The injection of 5, 10, or 50 mM $Ca^{2+}$ does not have any detectable mechanical effect (due to the absence of effect, we combine data points from all three $Ca^{2+}$ concentrations for each composition). Top: 100% DOPC ($N = 3$), centre: DOPC:DOPS = 9:1 ($N = 3$), bottom: DOPC:DOPS = 8:2 ($N = 10$). Refer to Table 1 for fitting parameters.

Interestingly, even in the absence of $Ca^{2+}$, charged membranes displayed low negative spontaneous curvature. Precisely, $R_0$, obtained from force measurements (Eq. 2) for reference 10% and 20% DOPS membranes, measured to be −120 nm and −200 nm, respectively (Table 1). We hypothesize two possible sources of the spontaneous curvature of charged membranes. First, the internal solution of vesicles is composed of pure sucrose, whereas the vesicles are immersed into a 100 mM NaCl buffer. Therefore, the repulsions of charged PS head groups are much less screened on the inner than the outer leaflet. As a result, the membrane tends to curve inward to alleviate this effect, hence generating negative curvature. Another possible contribution to spontaneous curvature is the insertion of $Na^+$ into the bilayer. A shallow insertion (just below the phosphate, Fig. 1A) would induce positive curvature, similar to the effect amphipathic protein helices have on the membrane[24]. Deeper penetration into the hydrocarbon core may, however, reverse the sign of curvature, as predicted by theory[24]. Considering that the effect is quite weak and is not affected by $Ca^{2+}$, we did not pursue its precise source.

It is still puzzling that $Ca^{2+}$, even at 50 mM does not impart any effect on 20% DOPS membranes. All experiments so far were performed in a 100 mM NaCl solution. If $Na^+$ indeed inserted deeply into the bilayer, as predicted by spontaneous curvature, it would be difficult to displace it with other ions.

We therefore repeated the experiment with 20% DOPS in the absence of NaCl. In this case, we observed a significant effect at 50 mM $Ca^{2+}$ to both the retraction force and the tether radius. Surprisingly, however, both force and radius decreased compared to the reference membrane (Fig. 3). It appears, contrary to our predictions based on the atomic structure, $Ca^{2+}$ generates positive membrane curvature, i.e. bends the bilayer toward the binding leaflet. Fitting Eq. 2 to the data yields reverse and approximately twice the magnitude of spontaneous curvature ($R_0 = +110$ nm) than the reference membrane in NaCl (Table 1).

It is generally assumed that the spontaneous curvature scales with the surface coverage of curvature-inducing particles[25, 26]. We can write this expression as:

$$\frac{1}{R_0} = \frac{1}{\tilde{R}_0}x \; , \tag{4}$$

where $\tilde{R}_0$ is the effective spontaneous curvature (intrinsic to the binding particle) and $x$ is the molar area fraction of bound $Ca^{2+}$. To calculate $x$, we use the Langmuir adsorption isotherm:

$$\frac{x}{1-x} = KC \ , \qquad (5)$$

where $C$ is the bulk ion concentration and $K$ the equilibrium binding constant. Taking $K = 650$ M$^{-1}$, as previously measured on 20% DOPS membrane[8], we obtain $x_{c=50mM} = 0.97$. Therefore, $\tilde{R}_0$ for Ca$^{2+}$ binding to 20% PS membranes is 107 nm, or 29 nm if calculated from fluorescence (the corresponding effective spontaneous curvatures are 0.009±0.009 nm$^{-1}$, or 0.035±0.0005 nm$^{-1}$ if calculated from fluorescence).
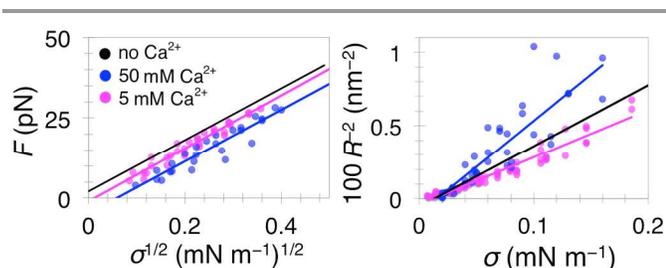


**Fig 3** Ca$^{2+}$ induces spontaneous curvature in the absence of NaCl. Fitting Eq. 2 (left) and Eq. 3 (right) to data obtained from DOPC:DOPS = 8:2 membrane in the presence of Ca$^{2+}$ at 5 mM ($N = 3$) and 50 mM ($N = 4$). Refer to Table 1 for fitting parameters.

Lower concentration of Ca$^{2+}$ (5 mM) induces five times lower, albeit still positive, curvature ($R_0 = +540$ nm). Compared to the size of the membrane, this value of spontaneous curvature is negligible and unlikely affects the morphology of the membrane. We list $R_0$ and $\kappa$ from all experiments in Table 1.

The observed positive spontaneous curvature is incompatible with our initial predictions based on lipid area contraction induced by Ca$^{2+}$ and with the proposed atomic coordination of Ca$^{2+}$ with the phosphodiester group[9, 15, 27, 28]. It seems that drawing an analogy with amphipathic protein helices, which insert below the phosphate, may be inaccurate. Instead, it is more likely that the strong repulsion between Ca$^{2+}$ ions, brought by their high charge density, becomes even stronger upon lipid area contraction. The perturbation is alleviated by generating positive curvature which will push Ca$^{2+}$ ions apart.

Taken together, we learn that NaCl strongly screens any mechanical effect on the membrane, even at 50 mM Ca$^{2+}$. It has been reported that Na$^{+}$ competes with divalent cations for the binding on PS-containing membranes[8] and, even on 100% PS membranes, it can replace Ca$^{2+}$ to a great extent[29]. To test the extent of electrostatic screening by NaCl, we performed $\zeta$-potential measurements on small liposomes composed of 20% DOPS. We offset the concentration of salts with glucose to prevent the osmotic shock. We find, in the absence of NaCl and Ca$^{2+}$, the potential to be $-57.6\pm2.4$ mV (mean±SD), however note that in the absence of electrolytes, this measurement is uncertain. In the presence of NaCl, due to electrostatic screening, there is a decrease in magnitude with increased NaCl concentrations (Fig. 4), measuring $-69.6\pm3.6$ mV (0.075 mM

NaCl), $-62.5\pm2.1$ mV (0.75 mM NaCl), $-59.4\pm1.9$ mV (10 mM NaCl), and $-52.4\pm1.9$ mV (20 mM NaCl), in good agreement with previously reported values[8, 30]. In the absence of NaCl, the $\zeta$-potential continuously rises with the concentration of Ca$^{2+}$, measuring $-30.4\pm0.9$ mV (0.05 mM Ca$^{2+}$), $-22.5\pm1.4$ mV (0.5 mM Ca$^{2+}$), $-10.9\pm0.5$ mV (5 mM Ca$^{2+}$), and $0.7\pm0.7$ mV (20 mM Ca$^{2+}$) (Fig. 4).

Finally, we measured the $\zeta$-potential in the presence of both ions. At 0.05 mM Ca$^{2+}$, we measured $-46.6\pm3.4$ mV (10 mM NaCl) and $-49.6\pm3.2$ mV (20 mM NaCl), whereas at 5 mM Ca$^{2+}$ the values were $-13.4\pm0.8$ mV (20 mM NaCl) and $-16.7\pm3.5$ mV (40 mM NaCl) (Fig. 4). It therefore appears that NaCl screens Ca$^{2+}$ relatively well at low concentrations (200–400 NaCl/Ca$^{2+}$ molar ratio). At high Ca$^{2+}$ concentrations (4–8 NaCl/Ca$^{2+}$ molar ratio) the $\zeta$-potential is also lower compared to NaCl-free conditions, however the screening effect is much weaker.
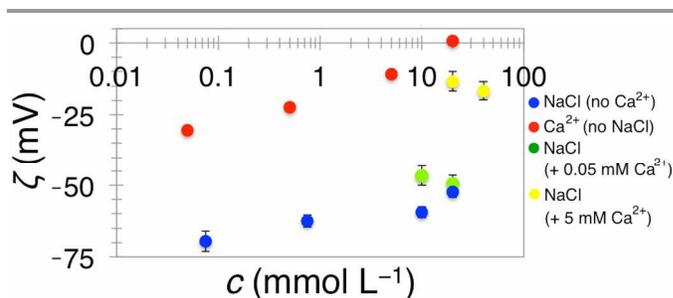


**Fig 4** $\zeta$-potential measurements of small liposomes (DOPC:DOPS = 8:2), as a function of salt concentration. Blue and red dots are measured in NaCl or Ca$^{2+}$, respectively. Green and yellow dots are measured in NaCl at a concentration indicated on the $x$-axis and it additionally contains, respectively, 0.05 or 5 mM Ca$^{2+}$.

**Table 1** Fitting parameters obtained from all experiments (mean±SD). Top values were obtained from force measurements using Eq. 2, whereas parenthetic values were obtained from fluorescence measurements using Eq. 3 and, in case of the radius, have an ambiguous sign.

| | DOPC | | 10% DOPS | | 20% DOPS | | 20% DOPS, no NaCl | |
|---|---|---|---|---|---|---|---|---|
| | no Ca | + $Ca^{2+}$ | no Ca | + $Ca^{2+}$ | no Ca | + $Ca^{2+}$ | +5 mM $Ca^{2+}$ | +50 mM $Ca^{2+}$ |
| $1/R_0$ (1/nm) | 1/3600±6E-5 (1/100±1E-3) | 1/350±2E-3 (1/50±2E-3) | −1/120±4E-3 (1/160±7E-4) | −1/60±8E-3 (1/90±6E-4) | −1/200±5E-3 (1/50±4E-4) | −1/160±6E-3 (1/60±4E-4) | 1/540±2E-3 (1/50±9E-5) | 1/110±9E-3 (1/30±5E-4) |
| $\kappa$ ($k_B T$) | 25.1±1.4 (22.2±1.5) | 29.9±7.0 (26.3±3.4) | 27.1±5.1 (9.7±0.7) | 20.0±3.9 (9.9±1.2) | 18.9±3.4 (12.4±1.1) | 23.4±4.5 (13.0±1.2) | 20.8±1.9 (15.0±0.5) | 19.9±2.9 (7.7±0.7) |

## Conclusions

Our single-vesicle essay shows that $Ca^{2+}$ ions induce positive spontaneous curvature on negatively charged membranes. We propose that the repulsion between $Ca^{2+}$ ions drives the membrane to curve outward, as to minimize their interactions. We also speculate that if $Ca^{2+}$ potentially drives the formation of PS domains, locally concentrating explicit charge would additionally result in positive spontaneous curvature. Our simple model predicts that $Ca^{2+}$ induces a positive radius of curvature on membranes with 20% net charge, with the magnitude of ~110 nm. This magnitude of curvature scales linearly with the bound coverage of $Ca^{2+}$, which depends on the bulk concentration and the amount of charged lipids in the bilayer. We note that there is a quantitative discrepancy between the calculated spontaneous curvature from independent force and fluorescence measurements. Both of these measurements have limitations, especially at high tension, where the radius is very thin and the force is very high, so it is difficult to predict which measurement provides a more accurate estimate of spontaneous curvature. Nevertheless, both measurements show qualitatively the same behavior in the presence and absence of NaCl, although fluorescence measurements systematically predict a lower radius of curvature.

What could be the consequences for a cell membrane? In cells, the concentration of $Ca^{2+}$ is very tightly controlled. While extracellular solution contains ~2.5 mM $Ca^{2+}$, the cytosolic concentration of $Ca^{2+}$ is normally kept at only nanomolar. It seems unlikely that $Ca^{2+}$ would induce a mechanical effect on a membrane of a quiescent cell. However, during various signaling events, its concentration may jump orders of magnitude and, combined with lipid clustering and area contraction, $Ca^{2+}$ could sufficiently locally cover the membrane to induce budding and tubulation. Such consequences would be undesirable in signal transduction phenomena. $Na^+$ ions completely inhibit the curvature effect of $Ca^{2+}$. Considering that our electrokinetic measurements revealed that $Ca^{2+}$ still alters the electrostatic environment of the membrane, curvature screening is not a consequence of electrostatic screening. Instead, we propose that the tight binding and deep insertion of $Na^+$ into the bilayer may serve as a very robust protection mechanism against nonspecific remodelling. Specialized proteins, such as those containing scaffolding domains, take the role of membrane sculptors, as they are specifically targeted to membrane remodeling sites[31, 32].

We hope our work will provide a better understanding of the extent of $Ca^{2+}$ ions affecting membrane mechanical properties at relevant concentrations of charge in the membrane and in the presence of physiological ionic strength.

## Materials and Methods

**Reagents.** 1,2-Dioleoyl-sn-glycero-3-phosphatidylcholine (DOPC), 1,2-dioleoyl-sn-glycero-3-phosphatidylserine (DOPS), and 1,2-distearoyl-sn-glycero-3-phosphoethanolamine-N-[biotinyl(polyethyleneglycol)-2000] (DSPE-PEG(2000)-biotin) were purchased from Avanti Polar Lipids. BODIPY-TR-C5-ceramide was purchased from Molecular Probes. All reagents used to make buffers and β-casein from bovine milk (>99%) were purchased from Sigma-Aldrich.

**Preparation of GUVs.** GUVs were prepared by electroformation on indium tin oxide glass[33]. DOPC and DOPS were mixed at desired molar ratio (see Results & Discussion) to which we added 0.5% BODIPY-TR-C5-ceramide and 0.03% DSPE-PEG(2000)-biotin (both molar percent). We smeared 10 μL of the mix (at 3 g/L) on each of the two slides of indium tin oxide glass, dried the film under vacuum for at least 1 h, then hydrated with sucrose. GUVs were grown under a sine voltage (1 V, 10 Hz) for approximately 1 h. The sucrose concentration was adjusted for each experiment so that the molalities of solutions inside and outside GUVs match.

**Tether-pulling experiment.** We followed the procedure described elsewhere[20, 21]. The experimental chamber and the aspiration pipette (~ 5 μm in diameter at the tip) were immersed for 30 min. in a solution of β-casein (5 g/L, dissolved in 100 mM NaCl, 10 mM HEPES) to minimize the adhesion of lipids to the glass surface. The chamber was then filled with the experimental solution (for experiments containing NaCl: 100 mM NaCl and 10 mM HEPES at pH = 7.4, and glucose to offset the molality inside GUVs; for saltless experiments: glucose with equal molality as the sucrose inside GUVs). Another pipette was filled with 10, 20, or 100 mM $CaCl_2$ (see Text) and offset if necessary with glucose to match the molality of the experimental solution. The chamber was sealed with oil after ~ 10 min. to prevent evaporation. GUVs with enough excess area to form an aspiration tongue[34, 35] were aspirated in a micropipette. Membrane tension was controlled via the aspiration pressure, using the Laplace relation:

$$\sigma = 0.5\Delta p r_p / (1 - r_p / r_v)$$

where $\Delta p$ is the hydrostatic pressure, $r_p$ and $r_v$ are radii of pipette and the vesicle, respectively[34]. A tether was created by bringing in contact the GUV with a streptavidin-coated polystyrene bead, ~ 3 μm in diameter (Spherotec), trapped with optical tweezers.

We measure the tether retraction force as: $F = k(a - a_0)$, where $a$ is the actual and $a_0$ the equilibrium position of the bead, tracked with bright field microscopy, $k$ is the stiffness of the trap, calibrated using the viscous drag method[36]. Typical measurement was performed by stepwise increasing the aspiration pressure and measuring the force and fluorescence for several minutes at each pressure. The measurement was then repeated by approaching the injection pipette and injecting $Ca^{2+}$, by either starting over from low pressure or reducing stepwise from high pressure. The direction of pressure did not affect the results (see Text). In experiments with no NaCl, we could only measure the steps after injecting $Ca^{2+}$, as the streptavidin-biotin interactions require the presence of ions. We conducted experiments by injecting 100 mM $Ca^{2+}$ (in the pipette, see above for the dilution factor) and incubating the vesicles with 5 mM $Ca^{2+}$. We measured the radius of the tether using the following relationship: $R = C_f I_t / I_v$, where $I_t$ and $I_v$ are the lipid fluorescence intensities of the tether and vesicle, respectively, and $C_f = 200 \pm 50$ is the calibration factor deduced previously[20].

We determined the dilution of the injected solution by injecting ~2 μM Alexa488 from a similar distance and injection pressure (10–20 Pa) as in all experiments with calcium. Alexa488 was bound to a membrane-binding protein, β2 centaurin, kindly provided by Harvey McMahon. We then measured the decrease in fluorescence intensity as a function of the distance from the pipette (three measurements). Keep in mind that assuming the same dilution factor for $Ca^{2+}$ as for the marker likely overestimates the near-vesicle concentration, considering that $Ca^{2+}$ has a lower hydrodynamic radius and it would diffuse out faster than the fluorescence marker. Taking the upper-limiting case ensures we do not overestimate the effect we quantify.

**Preparation of small liposomes.** The lipid mix composed of DOPC:DOPS (4:1, molar ratios), was dried under nitrogen to obtain 1 mg of dry mass. The mix was hydrated in 1 mL sucrose then freeze-thawed five times, followed by extrusion through a polycarbonate filter with pores 100 nm in diameter. We confirmed the final size of liposomes to be $106 \pm 7$ nm ($N = 4$) with dynamic light scattering.

**ζ-potential measurements.** We used a Malvern Zetaseizer NanoZS (Malvern Instruments Ltd.) to measure the electrophoretic mobility, which was converted to ζ-potential using Henry's equation $\zeta = 3u\eta / (2\varepsilon f)$ [37], where $u$ is the electrophoretic mobility, $\eta$ viscosity of the solution, $\varepsilon$ the dielectric constant, and $f$ Henry's function, calculated as [38]: $f = 1 + 0.5\left[1 + \left(2.5 / \lambda a\left[1 + 2e^{-\lambda a}\right]\right)\right]^{-3}$, where $a = 100$ nm was taken as the particle radius of curvature and $\lambda$ is the inverse Debye length, calculated as: $\lambda = \sqrt{\sum_{i=1}^{N} e^2 z_i^2 n_i / \varepsilon_r \varepsilon_0 k_B T}$. $N$ is the number of ionic species, $e$ is the elementary charge, $z_i$ and $n_i$ are charge number and amount of ion $i$, respectively, $\varepsilon_r$ and $\varepsilon_0$ are the relative and vacuum electric permittivity, $k_B$ is the Boltzmann constant, and $T$ the thermodynamic temperature[37]. For the case of pure glucose $f = 1.0$ was approximated. All measurements were taken three times.

## Bibliography

1. D. E. Clapham, *Cell*, 2007, **131**, 1047-1058.
2. M. E. Monteiro, M. J. Sarmento and F. Fernandes, *Biochem Soc Trans*, 2014, **42**, 1441-1446.
3. O. H. Petersen, M. Michalak and A. Verkhratsky, *Cell Calcium*, 2005, **38**, 161-169.
4. P. K. Tarafdar, H. Chakraborty, S. M. Dennison and B. R. Lentz, *Biophys J*, 2012, **103**, 1880-1889.
5. R. Ekerdt and D. Papahadjopoulos, *Proc Natl Acad Sci U S A*, 1982, **79**, 2273-2277.
6. T. Ito and S. I. Ohnishi, *Biochim Biophys Acta*, 1974, **352**, 29-37.
7. D. Papahadjopoulos, S. Nir and N. Duzgunes, *J Bioenerg Biomembr*, 1990, **22**, 157-179.
8. C. G. Sinn, M. Antonietti and R. Dimova, *Colloid Surface A*, 2006, **282**, 410-419.
9. P. T. Vernier, M. J. Ziegler and R. Dimova, *Langmuir*, 2009, **25**, 1020-1027.
10. I. Levental, A. Cebers and P. A. Janmey, *J Am Chem Soc*, 2008, **130**, 9025-9030.
11. M. Sovago, G. W. Wurpel, M. Smits, M. Muller and M. Bonn, *J Am Chem Soc*, 2007, **129**, 11079-11084.
12. R. A. Bockmann, A. Hac, T. Heimburg and H. Grubmuller, *Biophys J*, 2003, **85**, 1647-1655.
13. P. Mukhopadhyay, L. Monticelli and D. P. Tieleman, *Biophys J*, 2004, **86**, 1601-1609.
14. S. A. Pandit and M. L. Berkowitz, *Biophys J*, 2002, **82**, 1818-1827.
15. U. R. Pedersen, C. Leidy, P. Westh and G. H. Peters, *Biochim Biophys Acta*, 2006, **1758**, 573-582.
16. Y. H. Wang, A. Collins, L. Guo, K. B. Smith-Dupont, F. Gai, T. Svitkina and P. A. Janmey, *J Am Chem Soc*, 2012, **134**, 3387-3395.
17. H. Binder and O. Zschornig, *Chem Phys Lipids*, 2002, **115**, 39-61.
18. G. van Meer, D. R. Voelker and G. W. Feigenson, *Nat Rev Mol Cell Biol*, 2008, **9**, 112-124.
19. W. Helfrich, *Z Naturforsch C*, 1973, **28**, 693-703.
20. B. Sorre, A. Callan-Jones, J. Manzi, B. Goud, J. Prost, P. Bassereau and A. Roux, *Proc Natl Acad Sci USA*, 2012, **109**, 173-178.
21. H. F. Renard, M. Simunovic, J. Lemiere, E. Boucrot, M. D. Garcia-Castillo, S. Arumugam, V. Chambon, C. Lamaze, C. Wunder, A. K. Kenworthy, A. A. Schmidt, H. T. McMahon, C. Sykes, P. Bassereau and L. Johannes, *Nature*, 2015, **517**, 493-496.
22. K. Boesze-Battaglia and R. Schimmel, *J Exp Biol*, 1997, **200**, 2927-2936.
23. I. Derenyi, F. Julicher and J. Prost, *Phys Rev Lett*, 2002, **88**, 238101.
24. A. Zemel, A. Ben-Shaul and S. May, *J Phys Chem B*, 2008, **112**, 6988-6996.
25. S. Leibler, *J Phys-Paris*, 1986, **47**, 507-516.
26. R. Lipowsky, *Faraday Discuss*, 2013, **161**, 305-331; discussion 419-359.
27. J. M. Boettcher, R. L. Davis-Harrison, M. C. Clay, A. J. Nieuwkoop, Y. Z. Ohkubo, E. Tajkhorshid, J. H. Morrissey and C. M. Rienstra, *Biochemistry*, 2011, **50**, 2264-2273.
28. J. Seelig, *Cell Biol Int Rep*, 1990, **14**, 353-360.
29. R. Kurland, C. Newton, S. Nir and D. Papahadjopoulos, *Biochimica Et Biophysica Acta*, 1979, **551**, 137-147.
30. F. J. Carrion, A. Delamaza and J. L. Parra, *J Colloid Interf Sci*, 1994, **164**, 78-87.

ARTICLE

31.    H. T. McMahon and J. L. Gallop, *Nature*, 2005, **438**, 590-596.
32.    M. Simunovic and P. Bassereau, *Biol Chem*, 2014, **395**, 275-283.
33.    M. I. Angelova, S. Soléau, P. Méléard, F. Faucon and P. Bothorel, in *Trends in Colloid and Interface Science VI*, eds. C. Helm, M. Lösche and H. Möhwald, Steinkopff, 1992, vol. 89, pp. 127-131.
34.    R. Kwok and E. Evans, *Biophys J*, 1981, **35**, 637-652.
35.    D. Cuvelier, I. Derenyi, P. Bassereau and P. Nassoy, *Biophys J*, 2005, **88**, 2714-2726.
36.    K. C. Neuman and S. M. Block, *Rev Sci Instrum*, 2004, **75**, 2787-2809.
37.    A. V. Delgado, F. Gonzalez-Caballero, R. J. Hunter, L. K. Koopal and J. Lyklema, *J Colloid Interf Sci*, 2007, **309**, 194-224.
38.    H. Ohshima, *J Colloid Interf Sci*, 1994, **164**, 510-513.
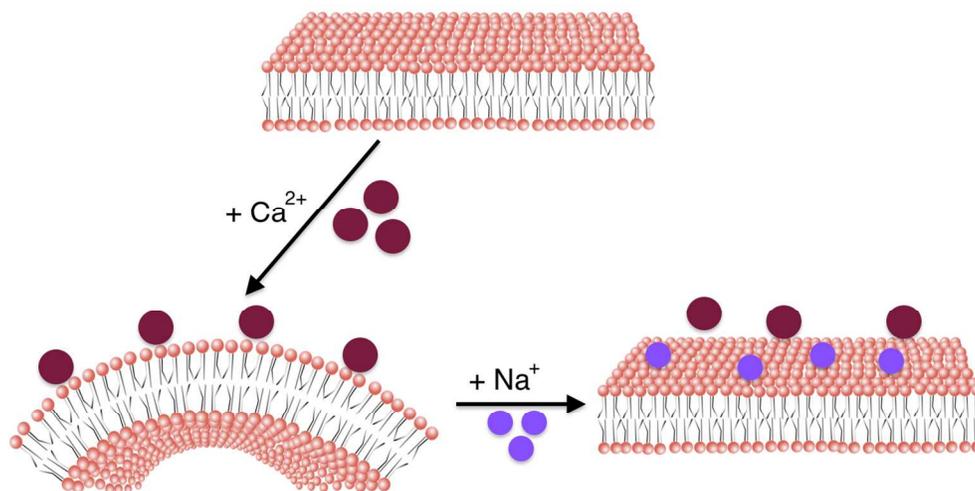
Calcium induces positive spontaneous curvature in negatively charged membranes, in a process completely screened by sodium.
538x276mm (72 x 72 DPI)